Eur Respir J 2008; 32: 1529–1539
DOI: 10.1183/09031936.00054608

Properties of a store-operated nonselective cation channel in airway smooth muscle

P.B. Helli*,# and L.J. Janssen*,#

ABSTRACT: Passive depletion of internal Ca^{2+} stores in airway smooth muscle (ASM) activates nonselective cation channels (NSCCs) that mediate capacitative Ca^{2+} entry. However, the single channel properties of these cation channels have yet to be resolved and their regulation by cytosolic Ca^{2+} levels ($[Ca^{2+}]_i$) still remains unclear.

NSCC currents and changes in $[Ca^{2+}]_i$ during passive depletion of internal Ca^{2+} stores were monitored in isolated bovine tracheal myocytes.

Loading cells with 1,2-bis(*o*-aminophenoxy)ethane-*N,N,N′,N′*-tetracetic acid acetyl methyl ester (BAPTA-AM) to reduce $[Ca^{2+}]_i$ and thereby deplete the store augmented a basal Gd^{3+}- and La^{3+}-sensitive, Ca^{2+}-permeable NSCC current. This current mimics that which is evoked by store depletion using the sarcoplasmic reticulum Ca^{2+} pump inhibitor cyclopiazonic acid (which concurrently and transiently elevates $[Ca^{2+}]_i$). Both interventions activated an ~25-pS NSCC with properties identical to both spontaneous (basal) and BAPTA-AM-evoked single channel currents.

In summary, the present study provides novel evidence that a lanthanide-sensitive, 25-pS nonselective cation channel underlies both basal and store depletion-evoked membrane currents in airway smooth muscle and that this conductance likely contributes to the regulation of resting $[Ca^{2+}]_i$ and capacitative Ca^{2+} entry.

KEYWORDS: Airway smooth muscle, BAPTA-AM, capacitative calcium entry, nonselective cation channel, single channel properties

Agonist-mediated bronchoconstriction involves release of Ca^{2+} from the sarcoplasmic reticulum (SR) [1–4]. The mechanisms responsible for store-refilling remain unclear but seem to include voltage-gated Ca^{2+} channels [5], nonselective cation channels (NSCCs) [1, 6, 7] and/or reverse-mode Na^+/Ca^{2+} exchange [8, 9]. NSCCs formed by proteins of the transient receptor potential (TRP) family have received a great deal of attention, particularly those of the ''canonical'' or ''classical'' subtype (TRPC) [10–12].

In airway smooth muscle (ASM), evidence of a functional link between TRPC expression and enhanced Ca^{2+}-influx (*i.e.* capacitative Ca^{2+} entry (CCE)) remains sparse. Recently, WHITE *et al.* [10] demonstrated that disruption of endogenous TRPC3 expression in human ASM reduced both resting cytosolic Ca^{2+} concentration ($[Ca^{2+}]_i$) and CCE; indirect pharmacological data suggested involvement of a NSCC but membrane currents were not measured directly. Indeed, only a few studies have directly examined store depletion-evoked membrane currents in ASM [1, 7, 13]. Hence, it is not surprising that their single channel properties have yet to be resolved. In addition, many previous studies of CCE were performed in the presence of agents which release stored Ca^{2+} (*e.g.* inositol triphosphate, caffeine) and/or which inhibit Ca^{2+} reuptake by the SR Ca^{2+} ATPase (SERCA; *e.g.* cyclopiazonic acid (CPA), thapsigargin) [7, 14–17]. However, these approaches elevate $[Ca^{2+}]_i$ [4, 14], which calls into question whether these currents are store depletion-activated or merely Ca^{2+} dependent since ASM is known to express NSCCs that are facilitated by elevated $[Ca^{2+}]_i$ [2, 6, 18]; in fact, the time course of activation of whole-cell NSCC currents by CPA in isolated bovine tracheal smooth muscle (TSM) cells paralleled the transient increase in $[Ca^{2+}]_i$ [7].

In order to better understand the relationship between store depletion, activation of NSCCs and regulation of $[Ca^{2+}]_i$ in ASM, activation of NSCC current during SR-depletion by loading the cells with the Ca^{2+} chelator 1,2-bis(*o*-aminophenoxy)ethane-*N,N,N′,N′*-tetracetic acid acetyl methyl ester (BAPTA-AM) was compared with inhibiting SERCA with CPA. The single channel properties of this conductance were also probed, as well as the contribution of this and other Ca^{2+}-permeable channels in mediating Ca^{2+} entry

AFFILIATIONS
*Dept of Medicine, McMaster University, and
#Firestone Institute for Respiratory Health, St. Joseph's Healthcare, Hamilton, ON, Canada.

CORRESPONDENCE
L.J. Janssen
St. Joseph's Hospital
room L314
50 Charlton Avenue East
Hamilton
ON
Canada
L8N 4A6
Fax: 1 9055406510
E-mail: janssenl@mcmaster.ca

Received:
April 09 2008
Accepted after revision:
June 26 2008

SUPPORT STATEMENT
These studies were supported by operating grants and a Career Award (L.J. Janssen) from the Canadian Institutes of Health Research (MOP 15561) and the Ontario Thoracic Society.

STATEMENT OF INTEREST
Statements of interest for both authors can be found at www.erj.ersjournals.com/misc/statements.shtml

European Respiratory Journal
Print ISSN 0903-1936
Online ISSN 1399-3003

upon SR Ca^{2+} depletion. Here, the present authors report that depletion of SR Ca^{2+} stores in the presence or absence of cytosolic Ca^{2+} transients activates an ~25-pS NSCC that contributes to resting $[Ca^{2+}]_i$, CCE and likely functions to refill internal Ca^{2+} stores in ASM.

MATERIALS AND METHODS

Tissues

All experimental procedures were approved by the McMaster University Animal Care Committee (McMaster University, Hamilton, ON, Canada) and conform to the guidelines set out by the Canadian Council on Animal Care (Ottawa, ON, Canada).

Trachea from commercial cattle (136–454 kg) were obtained at a local abattoir and transported in ice-cold Krebs' solution containing 116 mM NaCl, 4.6 mM KCl, 2.5 mM $CaCl_2$, 1.3 mM NaH_2PO_4, 1.2 mM $MgSO_4$, 23 mM $NaHCO_3$, 11 mM dextrose and 0.01 mM indomethacin, bubbled with 95% O_2/5% CO_2 in order to maintain a pH of 7.4. ASM was dissected free of epithelium and connective tissue and maintained in Krebs solution at 4°C for up to 48 h.

Cell isolation

Bovine TSM strips were gently agitated for 20 mins in modified Hank's balanced salt solution (with $NaHCO_3$, without $CaCl_2$ and $MgSO_4$) containing 2 $mg \cdot mL^{-1}$collagenase (Sigma blend type-F; Sigma-Aldrich, Oakville, ON, Canada) and 250 $\mu g \cdot mL^{-1}$ elastase (type-IV) at room temperature (21–23°C), then for an additional 20–40 mins at 37°C. Cells were dispersed by gentle trituration with a wide-bore pipette, centrifuged and resuspended in standard Ringer's solution containing 130 mM NaCl, 5 mM KCl, 1 mM $CaCl_2$, 1 mM $MgCl_2$, 20 mM HEPES, 10 mM dextrose and 0.1 mM niflumic acid (omitted for Ca^{2+} imaging) and adjusted to pH 7.4 with NaOH.

Electrophysiology

Single cells were allowed to adhere to the bottom of a recording chamber (1.5-mL volume) and then superfused with standard Ringer's solution at room temperature (21–23°C). Electrophysiological responses were tested in cells that were phase-dense and appeared relaxed. Average cell capacitance was 59 ± 5 pF (n=13).

Whole-cell currents were studied using the nystatin perforated patch configuration of the standard patch-clamp technique. Pipettes with tip resistances of 3–5 MΩ were fashioned from borosilicate glass. Tip potentials were nulled and electrophysiological recordings commenced, once series resistance dropped below 30 MΩ; 70–80% compensation was routinely employed. A holding potential of 0 mV was used to inactivate voltage-gated Ca^{2+} channels. Whole-cell currents were low-pass filtered at 1 kHz, sampled and digitised at 2.5 kHz (DigiData 1200 A/D converter; Axon Instruments, Foster City, CA, USA).

Liquid junction potentials between the electrode and bathing solutions were 3.5 ± 0.3 (n=6) and 11 ± 0.3 mV (n=4) for standard Ringer's and Na^+-free Ringer's solution, respectively; reversal potentials (Er) shown in the figures are not corrected whereas elsewhere they are corrected as previously described [7].

Pipettes with tip resistances of 7–13 Mohm were used to record single channel currents from on-cell patches. These currents were filtered at 5 kHz, sampled and digitised (at 20 kHz), and stored directly on a local hard-drive. Membrane potential was set to 0 mV by superfusing cells with a high molar KCl solution (see Solutions and Chemicals section). For offline analysis and figure preparation, single channel currents were filtered at 500 Hz. To evaluate single channel current-–voltage (I–V) characteristics, membrane potential was manually stepped from -120 to 60 mV. The transmembrane potential (V_m) is described by the equation:

$$V_m = V_{cell} - V_{pipette} \quad (1)$$

where V_{cell} is the membrane potential of the cell and $V_{pipette}$ is the potential imposed by the recording pipette. Assuming V_{cell} has been set to 0 mV by the external KCl solution, V_m is the negative of $V_{pipette}$. Inward channel currents are shown as downward deflections while outward currents are shown as upward deflections.

$[Ca^{2+}]_i$ fluorimetry

Single cells were incubated with fluo-4 AM (2 μM; containing 0.1% pluronic F-127) for 30 min at 37°C, then placed in a Plexiglas® recording chamber and superfused with Ringer's solution for 30 mins to allow for dye de-esterification. Confocal microscopy was performed at room temperature (21–23°C) as previously described [7]. Video images (600 × 400 pixels; Video Savant 4.0; IO Industries, London, ON, Canada) were generated at 1 $frame \cdot s^{-1}$ for caffeine responses and 0.1 $frame \cdot s^{-1}$ for all other responses. Average fluorescence intensities from regions of interest (30 × 30 pixels) defined in central non-nuclear regions of cells were calculated for each frame and plotted against time. Relative changes in $[Ca^{2+}]_i$ were expressed in terms of a change in fluorescence (ΔF) over the initial/baseline fluorescence (F_0) observed in the presence of 1.8 mM extracellular Ca^{2+}. Caffeine was applied directly to cells *via* pipette driven by a pressure ejection system (Picospritzer™ II; General Valve, Fairfield, NJ, USA).

Solutions and chemicals

All drugs and reagents were obtained from Sigma-Aldrich (Oakville, ON, Canada). Ca^{2+}-free Ringer's contained 130 mM NaCl, 5 mM KCl, 1 mM $MgCl_2$, 20 mM HEPES, 10 mM dextrose, 0.01 mM EGTA and 0.1 mM niflumic acid (omitted for Ca^{2+}-imaging), adjusted to pH 7.4 with NaOH. Na^+-free Ringer's solution consisted of 140 mM *N*-methyl-D-glucamine (NMDG), 5 mM KCl, 1 mM $CaCl_2$, 1 mM $MgCl_2$, 10 mM HEPES (adjusted to pH 7.4 with NaOH), 10 mM dextrose and 0.1 mM niflumic acid, adjusted to pH 7.4 with HCl. High molar KCl Ringer's solution contained 126 mM KCl, 1.5 mM $CaCl_2$, 1 mM $MgCl_2$, 10 mM HEPES, 10 mM dextrose and 0.1 mM niflumic acid adjusted to pH 7.4 with NaOH.

The intracellular electrode solution for measuring whole-cell currents contained 130 mM CsCl, 5 mM $MgCl_2$, 1 mM $CaCl_2$, 10 mM HEPES and 5 mM EGTA, adjusted to pH 7.2 with CsOH. These pharmacological and ionic conditions eliminated currents through Ca^{2+}-dependent Cl^- and K^+ channels. The standard electrode solution for on-cell recordings consisted of 126 mM NaCl, 1.5 mM $CaCl_2$, 10 mM HEPES and 10 mM

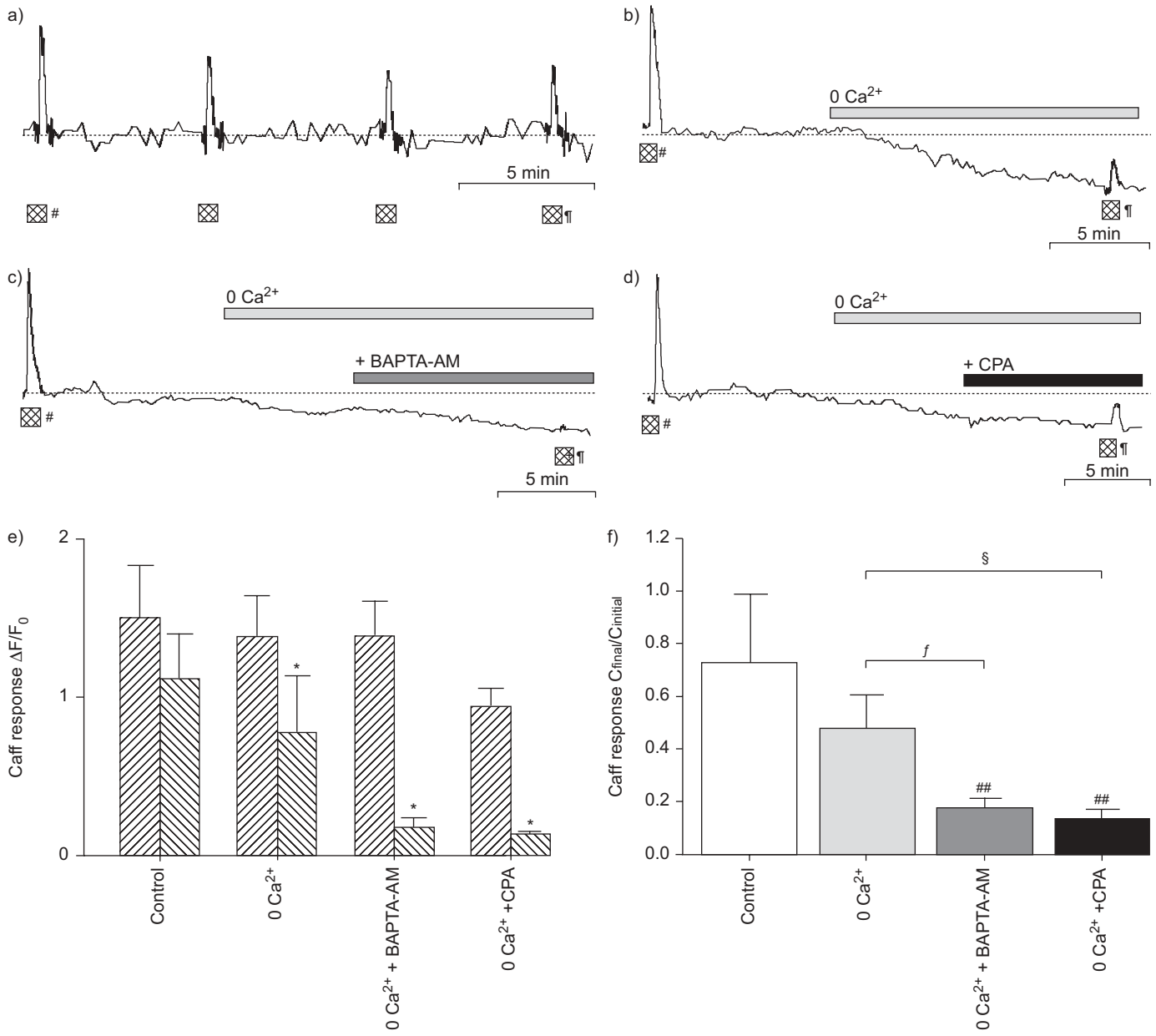

FIGURE 1. Effect of store depletion on cytosolic Ca^{2+} and sarcoplasmic reticulum Ca^{2+} concentration. a–d) representative fluorimetric traces illustrating effects of removal of extracellular Ca^{2+} (0 Ca^{2+}; ■), with or without concurrent treatment with: c) 10 μM BAPTA-AM (■) or d) 10 μM cyclopiazonic acid (CPA) on cytosolic Ca^{2+} concentration transients evoked by 10 mM caffeine (10 s application; ▩). Caffeine (caff) response mean data expressed both as: e) Change in fluorescence (ΔF)/baseline fluorescence (F_0) at initial response to caffeine ($C_{initial}$; ▨; # in a–d) and final response (C_{final}; ▧; ¶ in a–d) and f) $C_{final}/C_{initial}$ for control cells (n=10), 0 Ca^{2+} (n=9), 0 Ca^{2+} + BAPTA-AM (n=10) and 0 Ca^{2+} + CPA (n=8). ····: 0. *: $p<0.05$ *versus* initial response in same group, paired two-tailed t-test; ##: $p<0.05$ in a one-way ANOVA *versus* control. §: $p=0.028$; *f*: $p=0.03$.

dextrose, adjusted to pH 7.4 with NaOH. For high-Ca^{2+} electrode solution, NaCl was replaced by 70 mM $CaCl_2$. All on-cell electrode solutions were supplemented with 10 mM tetraethylammonium chloride, 5 mM 4-aminopyridine, 100 μM niflumic acid and 1 μM nifedipine to inhibit K^+-, Cl^-- and voltage-gated Ca^{2+} channels.

Nystatin for whole cell recordings was prepared in dimethyl sulphoxide (DMSO; 30 mg·mL^{-1}) for storage up to 5 days, and diluted to a final concentration of 300 μg·mL^{-1} in electrode solution daily. Reagents were dissolved in aqueous media (for Gd^{3+}, La^{3+}, caffeine) or DMSO (for CPA, BAPTA-AM, fluo-4 AM, nifedipine); the final concentration of DMSO in the bath was ⩽0.001% in all cases.

Data analysis

Whole-cell current records were obtained immediately before and during drug application with each cell acting as its own control. In studies where channel inhibitors were used, data are reported as % inhibition of BAPTA-AM evoked current prior to subtraction of baseline current.

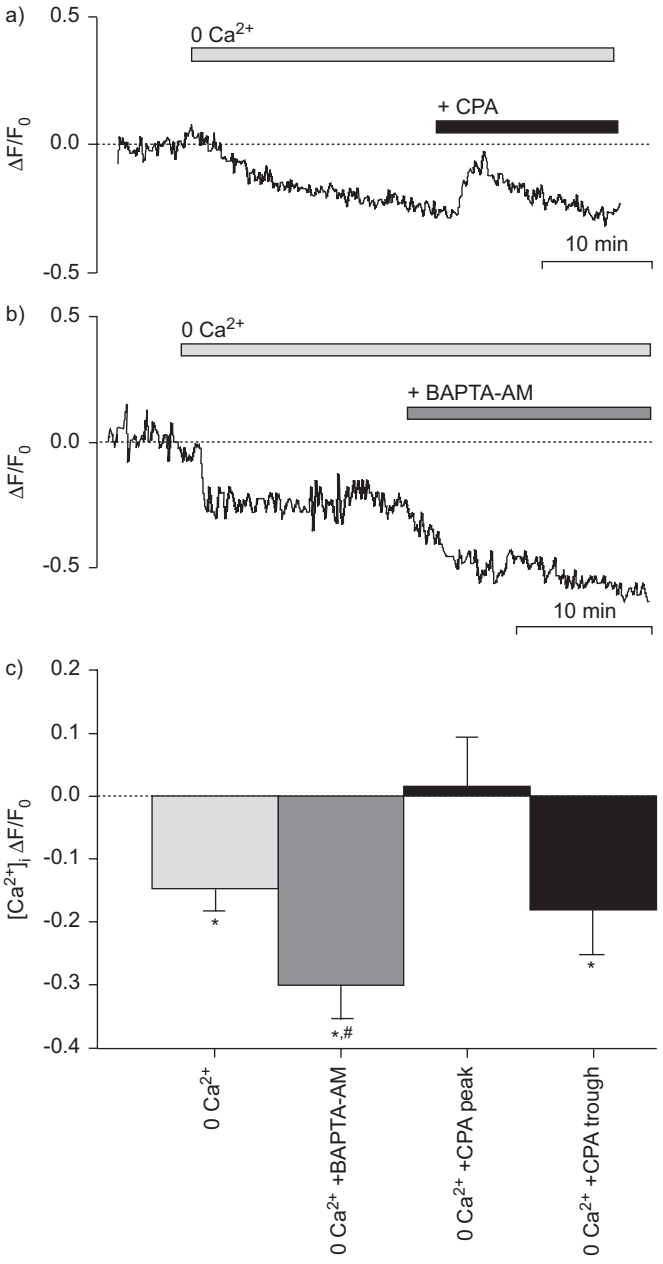

FIGURE 2. Representative traces illustrating changes in cytosolic Ca^{2+} concentration $[Ca^{2+}]_i$ following removal of extracellular Ca^{2+} (0 Ca^{2+}; ■) followed by inhibition of the sarcoplasmic reticulum Ca^{2+} ATPase with 10 μM cyclopiazonic acid (CPA) or passive loading with 10 μM BAPTA-AM in bath. c) mean change in $[Ca^{2+}]_i$ (n=12–35). ····: 0. *: $p<0.05$, change in $[Ca^{2+}]_i$ from baseline (F_0). #: $p<0.05$ *versus* 0 Ca^{2+}, one-way ANOVA.

Unitary current amplitude histograms for individual patches were constructed from 0.5–2-s sections of raw traces. I–V relationships, from individual patches in which unitary channel current amplitudes were measured at a minimum of three different membrane potentials, were plotted and the unitary conductance and Er for individual patches were then calculated using linear regression (least-squares method). The mean unitary conductance and Er were determined by averaging values from individual patches.

All data are reported as means±SEM, n values indicate number of animals tested; comparisons were made using a paired or unpaired t-test or one-way ANOVA as appropriate, with p-values <0.05 considered significant.

RESULTS

Differential effects of store depletion protocols on $[Ca^{2+}]_i$ and SR Ca^{2+} content

$[Ca^{2+}]_i$ responses evoked by a 10-s application of 10 mM caffeine were utilised as an index of SR Ca^{2+} content. In the presence of 1.8 mM extracellular Ca^{2+}, repetitive caffeine stimulations at 5-min intervals evoked reproducible transient $[Ca^{2+}]_i$ elevations (fig. 1a–d). In contrast, bathing cells in Ca^{2+}-free Ringer's solution for 10 mins, reduced baseline $[Ca^{2+}]_i$ ($\Delta F/F_0 = -15\pm3$, n=35; $p<0.001$) and decreased the magnitude of caffeine-evoked transients by 52±13% (n=9; p=0.027), suggesting that basal Ca^{2+} entry is necessary for the maintenance of resting $[Ca^{2+}]_i$ and SR Ca^{2+} loading. L-type Ca^{2+} channels did not mediate this basal Ca^{2+} entry, since 1 μM nifedipine did not significantly reduce baseline fluorescence ($\Delta F/F_0 = 0.6\pm0.6$, n=10, data not shown).

Both CPA and BAPTA-AM (10 μM each) further reduced SR Ca^{2+} content such that caffeine-evoked $[Ca^{2+}]_i$ responses were reduced to a much greater extent than was seen following removal of extracellular Ca^{2+} alone (fig. 1a–d). In the absence of extracellular Ca^{2+}, application of CPA evoked a transient rise in fluorescence, followed within 10 mins by a sustained decrease to pre-drug levels (fig. 2); the rise in $[Ca^{2+}]_i$ likely reflecting Ca^{2+} leak from the SR *via* ryanodine receptors, while the return to baseline involves Ca^{2+} extrusion *via* the plasmalemmal Ca^{2+} pump [4, 5, 14, 19]. In contrast, treating cells with BAPTA-AM following removal of external Ca^{2+} caused a further decline in $[Ca^{2+}]_i$ that stabilised within 10–15 mins (fig. 2).

Loading with BAPTA-AM activates a NSCC in bovine TSM cells

In cells held under voltage-clamp, a small membrane current with mean amplitude of -82±19 pA at -60 mV was observed. BAPTA-AM markedly increased the amplitude of this current, which was stable for >30 mins (fig. 3). Voltage steps from -80 mV to 60 mV (10 mV increments, 200 ms duration, from a holding potential of 0 mV) elicited currents that showed little time-dependent activation except at very negative potentials and no deactivation over the 200 ms period of the voltage step (fig. 3). The steady-state I–V relationship of both the baseline membrane current and BAPTA-AM-evoked current were linear with Er of 5.4±2.2 and -1.5±1.5 mV respectively (n=14; fig. 3). Instantaneous I–Vs obtained using ramp voltage commands (-100 to 80 mV, 2-s duration, from a holding potential of 0 mV) were identical (*cf.* fig. 4d).

Replacement of extracellular Na^+ with NMDG substantially reduced the inward portion of the BAPTA-AM-dependent current (fig. 4) such that the I–V relationship was best described by a quadratic equation and Er was displaced from -3.8±2.4 mV to -21±1.2 mV (n=4), representing a shift of -17 mV (95% confidence interval (CI) of -13– -21 mV) as would be expected if Na^+ were a major charge carrier for this conductance.

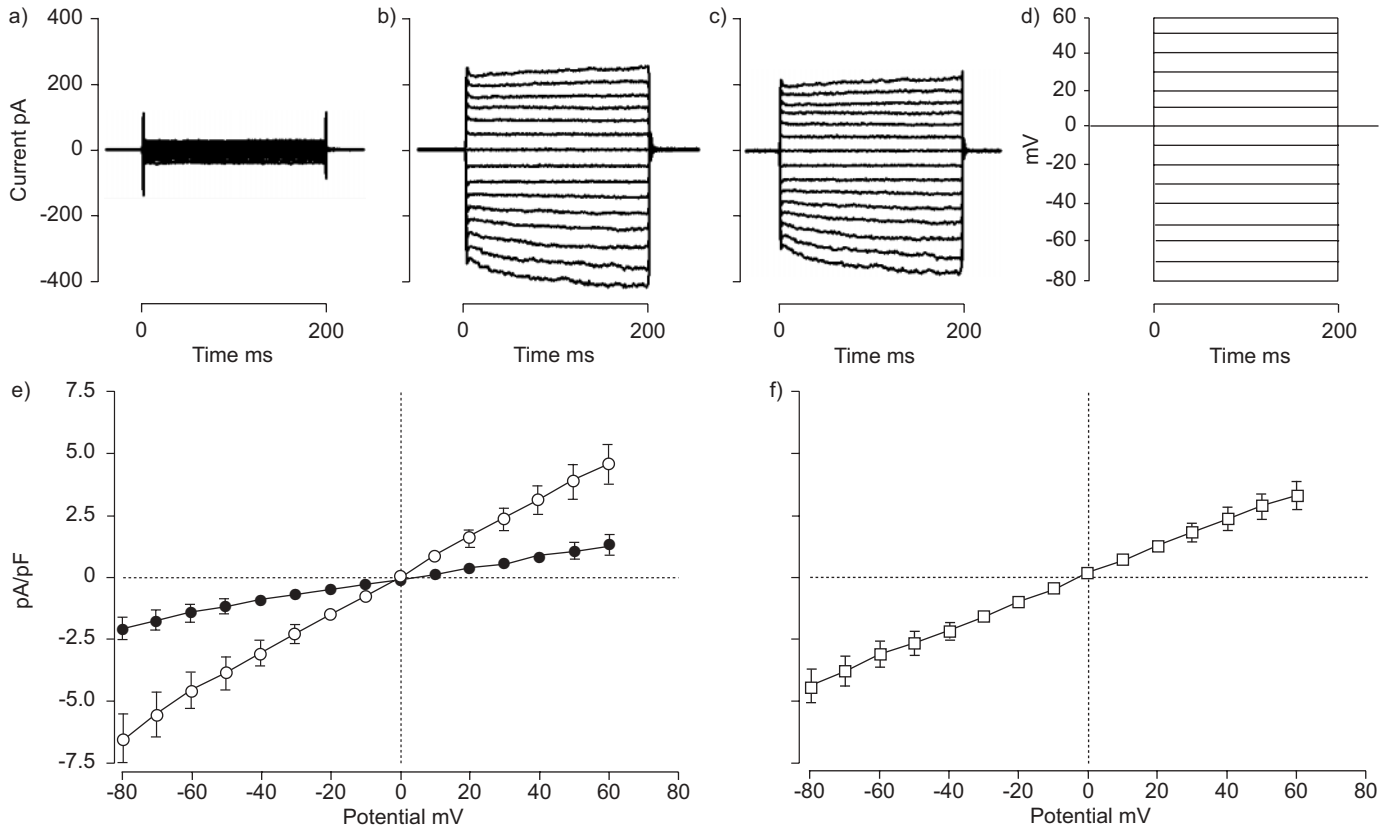

FIGURE 3. Store depletion by BAPTA-AM augments a basal nonselective cation channel current. Representative traces of membrane currents evoked by voltage step pulses (200 ms duration, 10 mV increments as shown in d) delivered from a holding potential of 0 mV before (a) and after (b) application of 10 μM BAPTA-AM; the difference in current is also shown (c). e) Mean currents obtained prior to (●) and during application of BAPTA-AM (○; n=13). f) Difference (□) between before and during application of BAPTA-AM. ····: 0.

Next, the pharmacology of the BAPTA-AM-activated current in these cells was examined by addition of blockers to the bathing medium (results summarised in table 1). La^{3+}, which inhibits CCE in several ASM preparations [10, 16, 20], reduced BAPTA-AM-evoked membrane currents but did not shift Er (fig. 5); this effect was concentration dependent and poorly reversible. Alternatively, 10 μM Gd^{3+} (which has been widely utilised as an inhibitor of NSCCs and CCE in several smooth muscle cell types [21–23]) had little effect on the BAPTA-AM-evoked current, although 100 μM caused a marked and irreversible suppression (fig. 5).

Cell attached patches exhibit spontaneous single channel activity

In order to better understand the nature of the channel responsible for mediating resting and store-depletion evoked whole-cell membrane currents in bovine TSM cells, single channel events recorded from cell-attached patches were examined. Using high-K^+ Ringer's solution to clamp Vm around 0 mV and a pipette solution containing 126 mM NaCl and 1.5 mM Ca^{2+}, discrete single channel openings were recorded at both positive and negative transmembrane potentials (fig. 6a). In eight of the 18 cells examined, these spontaneous events were sufficiently frequent to allow for analysis of unitary current amplitudes; the I–V relationship of the spontaneous single channel currents had a slope-conductance of 26±0.3 pS with Er= -2±3 mV (n=4; fig. 6e). When studied with a patch pipette containing 70 mM $CaCl_2$ the slope conductance was unchanged (24±2 pS) but the Er was shifted leftward -14 mV (p=0.024, n=4; fig. 6e), indicative of a high permeability to Na^+.

CPA and BAPTA-AM evoke single channel activity in previously quiescent patches

In membrane patches exhibiting little evidence of spontaneous single channel activity, treatment with 10 μM CPA or 10 μM BAPTA-AM substantially increased the number of single channel events (figs 7 and 8). The I–V relationships for these unitary events were linear in nature, with a slope-conductance of 23±1 and 26±1 pS and Er occurring at -5±3 and -6±1 mV for CPA (n=7) and BAPTA-AM (n=3), respectively (126 mM NaCl electrode and 140 mM KCl bathing solution; fig. 8). When studied with a 70 mM $CaCl_2$ pipette solution, the slope conductance and Er of the CPA-evoked single channel current was 20±1 pS and -10±5 mV (n=3), respectively. The similarities in the properties of the spontaneous, CPA- and BAPTA-AM-evoked single channel currents, as well as the similarity of their I–V relationship with that of the whole cell current, suggests that the same NSCC underlies all three.

DISCUSSION

In many smooth muscle cell types, agonists release Ca^{2+} from an intracellular Ca^{2+} store [6, 16, 23]. Subsequent restoration of

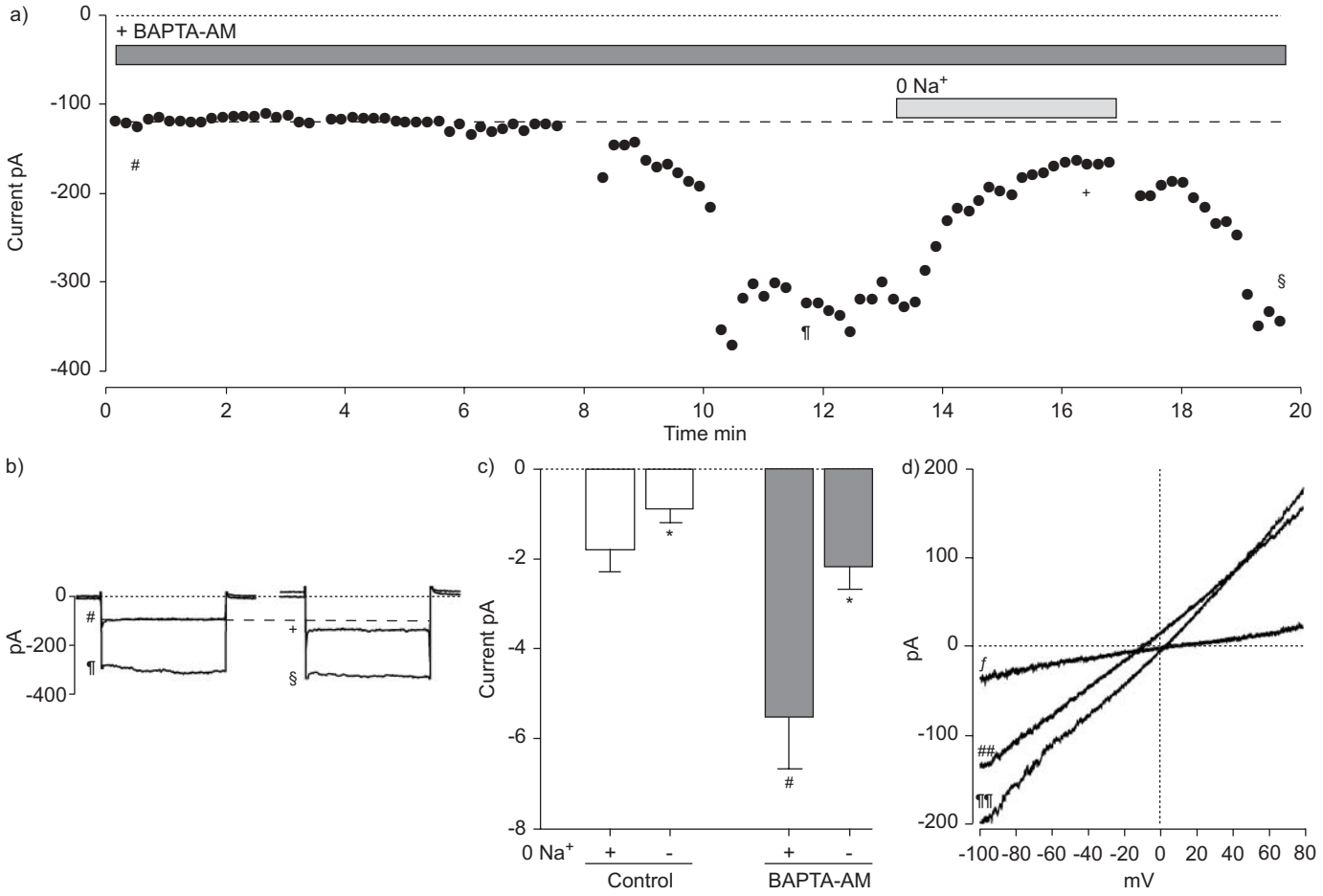

FIGURE 4. Effect of removing external Na^+ on basal and BAPTA-AM-evoked nonselective cation channel currents. a) time course of BAPTA-AM-evoked (■) whole-cell current. Mean current (●) observed upon voltage stepping cell to -60 mV from a holding potential of 0 mV (200 ms duration, 10 s intervals). Extracellular Na^+ in the bathing medium (flow rate of ~3 mL·min^{-1}) was replaced with equimolar *N*-methyl-D-glucamine (NMDG; ■). b) current traces from the cell shown in a at time-points $^{\#}$, ¶, $^{+}$ and §. c) mean basal (□, n=5) and BAPTA-AM-evoked (■, n=4) current at -60 mV before (-) and after (+) replacement of extracellular Na^+ (0 Na^+). d) basal (^{f}) and BAPTA-AM-evoked membrane currents in the presence of Na^+ (¶¶) or following replacement with NMDG ($^{\#\#}$) obtained from a single cell studied using a voltage ramp from -100 mV to 80 mV over 2 s. ·····: 0; ------: basal current. *: $p<0.05$ reduction upon removal of Na^+; $^{\#}$: $p<0.05$, one-way ANOVA *versus* control.

$[Ca^{2+}]_i$ includes both re-uptake into the store by SERCA as well as extrusion from the cell by the plasmalemmal Ca^{2+} pump and/or Na^+/Ca^{2+} exchanger. As such, there must be mechanisms in place to compensate for the net loss of cellular Ca^{2+} in order to avoid complete depletion of the store. In ASM, it appears that CCE, mediated by NSCCs, may be involved [1, 5, 7, 13]; however there are many unresolved issues regarding the electrophysiological properties, regulation and physiological roles of these channels. The present study examined the properties of a membrane conductance activated by store depletion through either chelation of intracellular Ca^{2+} with BAPTA or inhibition of SERCA with CPA. In addition, the relative contribution of this channel in regulating $[Ca^{2+}]_i$ and CCE was also examined, with the goal of generating a better understanding of the ionic mechanisms underlying CCE in ASM. Notably, novel data regarding the single channel characteristics of this conductance are presented.

TABLE 1 Pharmacological profile of BAPTA-AM-evoked membrane current in bovine tracheal smooth muscle cells measured at -60 mV.

Inhibitor	BAPTA-AM-evoked current inhibition %	n
Gd^{3+}		
10 μM	35±15	6
100 μM	80±5*	6
La^{3+}		
1 μM	28±15	4
10 μM	65±8*	5
100 μM	82±3*	5

Data are presented as mean±SEM. *: $p<0.05$ from one-tailed paired t-test.

Many of the isolated bovine TSM cells displayed NSCC currents at rest (*i.e.*, prior to store depletion); this has been described previously [7]. NSCCs in ASM, whether activated by G-protein coupled receptor stimulation [6] or by passive depletion of SR Ca^{2+} (present study and [7]), are highly permeable to Na^+, conducting a significant inward Na^+ current

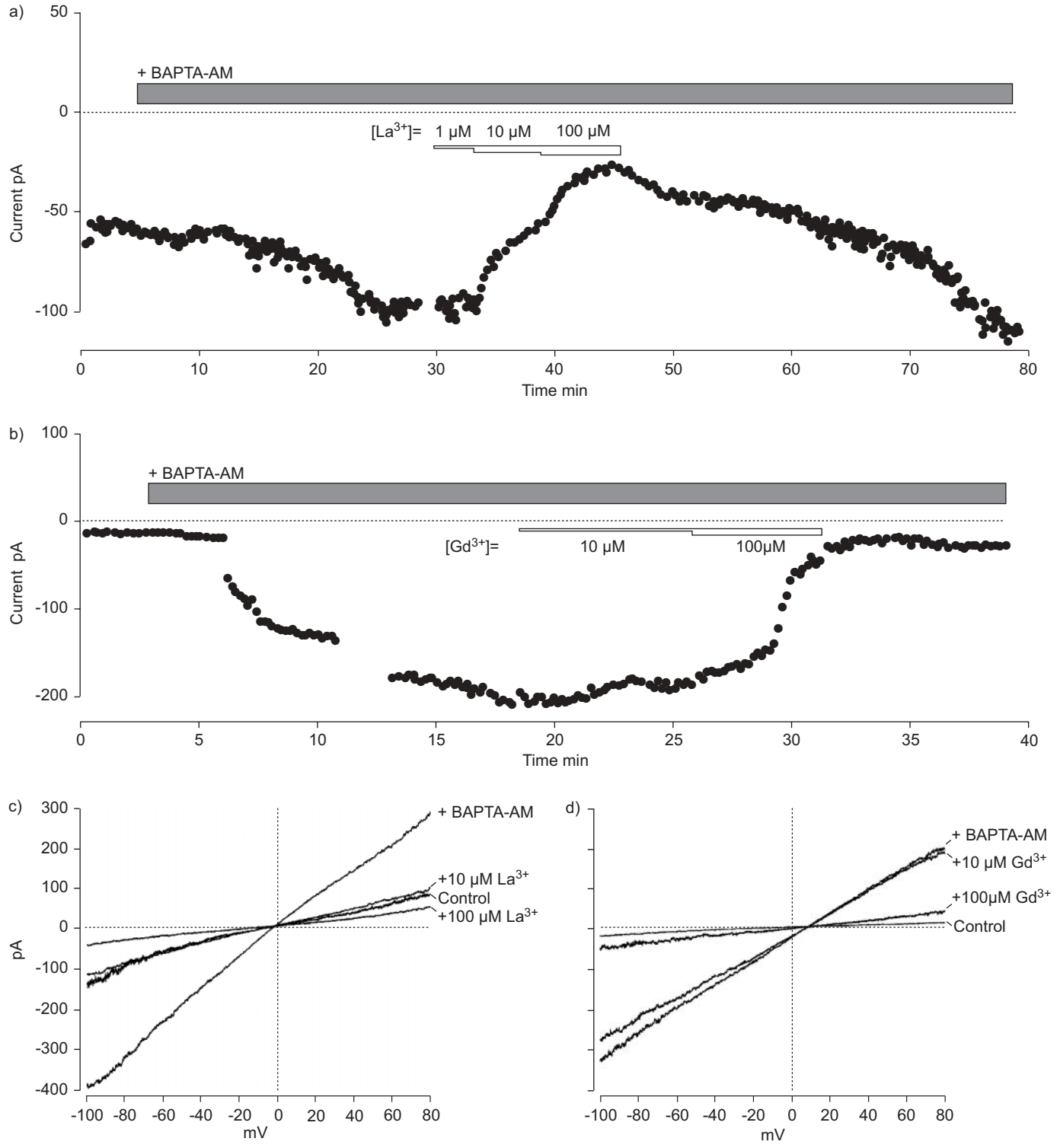

FIGURE 5. Block of BAPTA-AM-evoked whole-cell current by La^{3+} and Gd^{3+}. Time course of inhibition of BAPTA-AM-evoked (■) membrane current by a) La^{3+} or b) Gd^{3+} in two separate cells. The amplitude of inward membrane currents elicited by voltage stepping cells to -60 mV at 10-s intervals is shown (●). Representative traces of membrane currents studied using voltage ramps in two separate cells. c) La^{3+} and d) Gd^{3+} were added to the bathing solution following activation of membrane current by 10 µM BAPTA-AM. ····: 0.

across a range of physiologically relevant membrane potentials (*e.g.* -60 to -30 mV). A large portion of the baseline and BAPTA-AM-evoked NSCC currents in the present study were also dependent upon extracellular Na^+ (fig. 4). These channels are also known to conduct Ca^{2+}. Although one estimate found this to comprise only 14% of the overall current, it is sufficient

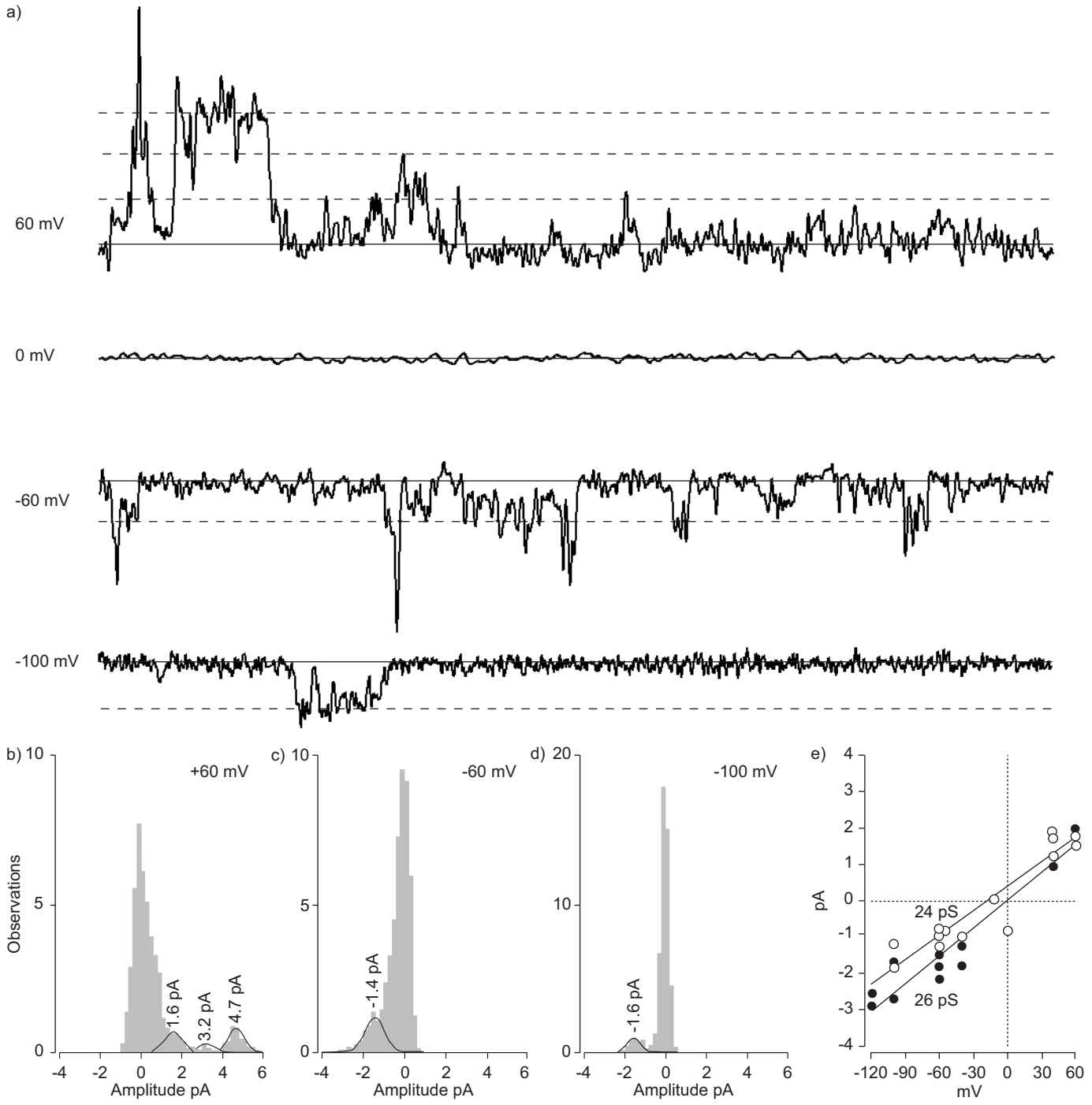

FIGURE 6. Properties of spontaneous unitary nonselective cation channel events. a) Representative traces of spontaneous single channel currents observed in a cell-attached patch (126 mM $NaCl_2$ electrode) at different potentials. —: closed channel state; - - -: predicted open states. All-points histograms for the data presented in (a) at b) 60 mV, c) -60 mV and d) -100 mV. e) Mean current–voltage plots for spontaneous unitary channel currents studied with pipettes containing 126 mM NaCl (●; n=4) or 70 mM $CaCl_2$ (○; n=4). ····: 0.

to maintain a modest yet sustained elevation of $[Ca^{2+}]_i$ [2, 6]. Others have demonstrated a constitutively active, nifedipine-insensitive Ca^{2+} influx pathway in bovine TSM, which is speculated to contribute to a resting $[Ca^{2+}]_i$ around 100-150 nM [14, 20]. CPA enhances Ca^{2+} entry in several other ASM preparations presumably through activation of Ca^{2+}-permeable NSCCs [10, 15, 16, 24]. Basal NSCC currents have also been described in isolated smooth muscle cells from rabbit portal vein [25], ear artery [26] and coronary artery [22] as well as rat pulmonary artery [27].

The signalling pathway underlying activation of the store-operated NSCC currents is unclear. In the present study, G-protein coupled receptor signalling was not necessary for

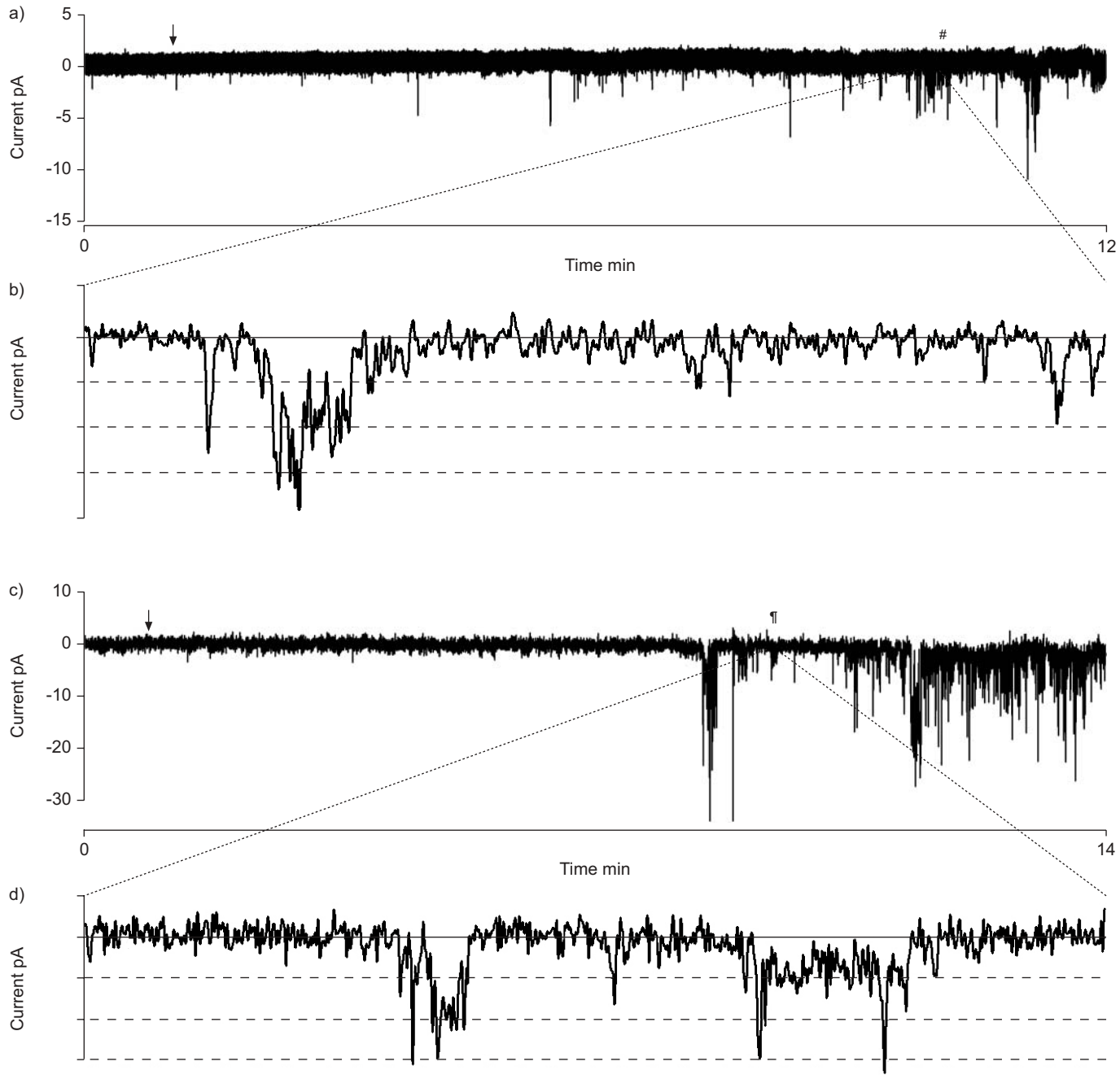

FIGURE 7. Properties of cyclopiazonic acid (CPA) and BAPTA-AM-evoked single channel currents. Representative traces of single channel membrane currents induced by bath application (arrow) of 10 μM a) CPA or c) BAPTA-AM at a transmembrane potential of -60 mV. The 500 ms portions (#, ¶) of recordings are expanded in b) and d) for CPA and BAPTA-AM, respectively. ——: closed channel state; - - -: predicted open channel states. Pipettes contained 70 mM $CaCl_2$ (a, b) and 126 mM NaCl (c, d).

NSCC activation, since treatment with BAPTA-AM or CPA alone was sufficient, although the possibility that this current may be regulated through diacylglycerol–protein kinase C-dependent mechanisms as demonstrated in vascular smooth muscle [28] cannot be ruled out. Also, although Ca^{2+}-dependent facilitation of NSCC currents has been described in equine [2, 6] and porcine [18] TSM, the possibility that this channel was merely regulated by Ca^{2+} or Ca^{2+}-dependent mechanisms is unlikely, since CPA evokes a transient increase in $[Ca^{2+}]_i$ [7] whereas BAPTA-AM suppresses $[Ca^{2+}]_i$.

In rabbit portal vein myocytes, spontaneous and store depletion-activated single channel events exhibit identical properties including unitary conductance, E_r and mean open times, suggesting that a similar channel underlies both currents [25]. To determine if a similar mechanism operates in ASM, on-cell measurements of single channel currents were conducted both prior to and during passive store depletion with either CPA or BAPTA-AM. In all cell-attached patches examined, there was evidence of spontaneous single channel activity (~44% exhibiting robust activity), which was

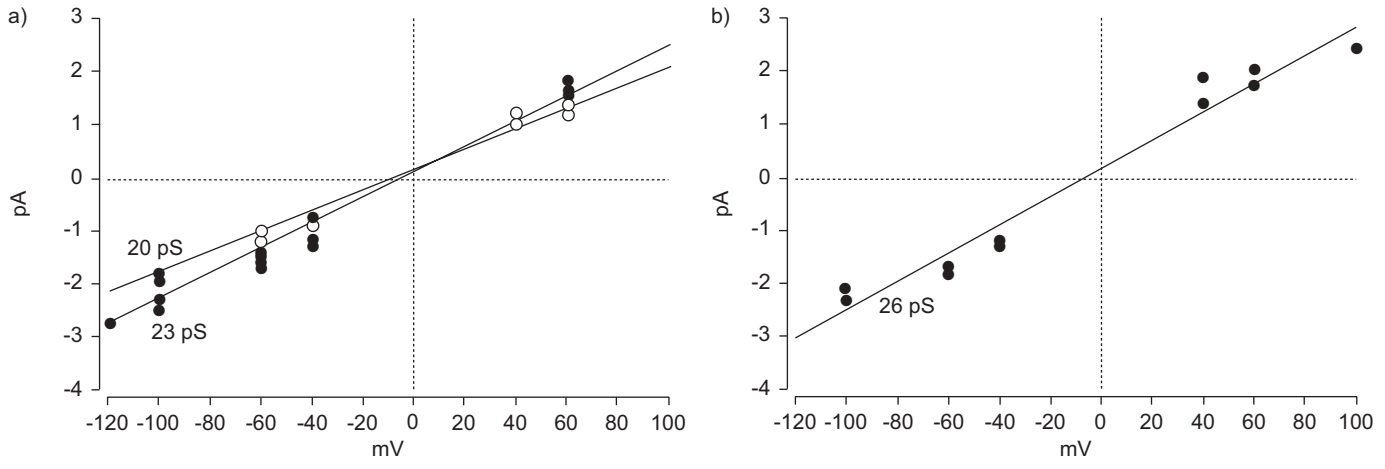

FIGURE 8. Mean current–voltage plots for a) cyclopiazonic acid (CPA) and b) BAPTA-AM-evoked unitary channel currents measured with pipettes containing 126 mM NaCl (●; n=7 and n=4 for CPA and BAPTA-AM, respectively) or 70 mM $CaCl_2$ (○; n=3).

attributed to a NSCC, given that the conductance was permeable to Na^+ and Ca^{2+} and that membrane currents through Ca^{2+}-regulated Cl^- channels, voltage-operated K^+ channels, Ca^{2+}-regulated K^+ channels and voltage-operated Ca^{2+} channels were eliminated by experimental design. Application of CPA or BAPTA-AM greatly increased the frequency and number of unitary channel events observed; single channel analysis revealed this to be mediated by a unitary conductance of ~25 pS. The lanthanides Gd^{3+} and La^{3+} inhibit CPA-activated membrane currents and/or CCE in several tissues [16, 21, 27]. In the present study, application of 10 and 100 μM La^{3+} reversibly inhibited the BAPTA-AM-evoked current in a dose-dependent manner. This current was also found to be largely resistant to 10 μM Gd^{3+}, although 100 μM Gd^{3+} caused a marked reduction of ~80%. In contrast to La^{3+}, the inhibitory effect required several minutes to develop fully and was irreversible. It has been similarly found that extracellular Gd^{3+} irreversibly blocks TRP3 currents in Chinese hamster ovary cells with a late onset [29]; the authors of that study speculated that the kinetics of inhibition by Gd^{3+} in intact cells relied upon the uptake and extrusion rate of this cation, since the median effective concentration (EC_{50}) was lower and the rate of inhibition faster when Gd^{3+} was applied to the cytosolic face of the channel.

While others have shown that a 25 pS NSCC with similar properties (*i.e.*, unitary conductance and sensitivity to 1 mM La^{3+}, Gd^{3+} and 100 μM SKF 96365) is activated by leukotrienes in isolated human BSM, its role in mediating CCE was not specifically examined [3]. As such, the current finding that an ~25 pS channel underlies CPA- and BAPTA-AM-evoked NSCC currents in bovine TSMs is novel. The magnitude of the conductance described herein is 10-fold greater than that reported for store depletion-activated NSCCs in vascular smooth muscle cells [25, 30, 31]; the possibility that small conductance NSCCs were hidden within the noise inherent in the recordings cannot be ruled out. Involvement of this NSCC explains why the Ca^{2+} entry induced by CPA was resistant to nifedipine (fig. 6). BAZAN-PERKINS *et al.* [20] found that the rate of Ca^{2+} entry in bovine TSM cells with depleted SR Ca^{2+} stores was resistant to D600. Likewise, in guinea pig TSM, depletion of SR Ca^{2+} with the SERCA inhibitor thapsigargin induced a rise in $[Ca^{2+}]_i$ and a contraction that was dependent upon extracellular Ca^{2+}, was inhibited by Ni^{2+} and SKF 96365 but not nifedipine [15], and similar results have been observed in rat basolateral membrnae upon depletion of acetylcholine-sensitive stores [1].

In summary, the present authors conclude that loading of bovine tracheal smooth muscle cells with BAPTA-AM (in order to reduce cytosolic Ca^{2+} concentration and thereby deplete the store) augments a basal, Ca^{2+}-permeable nonselective cation conductance that is both Gd^{3+}- and La^{3+}-sensitive. In addition, the present findings indicate that an ~25 pS nonselective cation channel underlies both basal, cyclopiazonic acid- and BAPTA-AM-evoked membrane currents in this tissue. Furthermore, the data suggest that nonselective cation channels contribute to the regulation of cytosolic Ca^{2+} concentration and sarcoplasmic reticulum refilling and are likely to be responsible for the capacitative Ca^{2+} entry observed in airway smooth muscle.

REFERENCES

1 Sweeney M, McDaniel SS, Platoshyn O, *et al.* Role of capacitative Ca^{2+} entry in bronchial contraction and remodeling. *J Appl Physiol* 2002; 92: 1594–602.
2 Wang YX, Kotlikoff MI. Signalling pathway for histamine activation of nonselective cation channels in equine tracheal myocytes. *J Physiol* 2000; 523: 131–138.
3 Snetkov VA, Hapgood KJ, McVicker CG, Lee TH, Ward JP. Mechanisms of leukotriene D4-induced constriction in human small bronchioles. *Br J Pharmacol* 2001; 133: 243–252.
4 Janssen LJ, Wattie J, Lu-Chao H, Tazzeo T. Muscarinic excitation-contraction coupling mechanisms in tracheal and bronchial smooth muscles. *J Appl Physiol* 2001; 91: 1142–1151.
5 Janssen LJ, Sims SM. Emptying and refilling of Ca^{2+} store in tracheal myocytes as indicated by ach-evoked currents and contraction. *Am.J.Physiol* 1993; 265: C877–C886.

6 Fleischmann BK, Wang YX, Kotlikoff MI. Muscarinic activation and calcium permeation of nonselective cation currents in airway myocytes. *Am J Physiol* 1997; 272: C341–C349.
7 Helli PB, Pertens E, Janssen LJ. Cyclopiazonic acid activates a Ca^{2+}-permeable, nonselective cation conductance in porcine and bovine tracheal smooth muscle. *J Appl Physiol* 2005; 99: 1759–1768.
8 Hirota S, Pertens E, Janssen LJ. The reverse mode of the Na^{+}/Ca^{2+} exchanger provides a source of Ca^{2+} for store refilling following agonist-induced Ca^{2+} mobilization. *Am J Physiol Lung Cell Mol Physiol* 2007; 292: L438–L447.
9 Dai JM, Kuo KH, Leo JM, van Breemen C, Lee CH. Mechanism of ACh-induced asynchronous calcium waves and tonic contraction in porcine tracheal muscle bundle. *Am J Physiol Lung Cell Mol Physiol* 2006; 290: L459–L469.
10 White TA, Xue A, Chini EN, Thompson M, Sieck GC, Wylam ME. Role of transient receptor potential C3 in TNF-α-enhanced calcium influx in human airway myocytes. *Am J Respir Cell Mol Biol* 2006; 35: 243–251.
11 Freichel M, Vennekens R, Olausson J, *et al*. Functional role of TRPC proteins in native systems: implications from knockout and knock-down studies. *J Physiol* 2005; 567: 59–66.
12 Albert AP, Pucovsky V, Prestwich SA, Large WA. TRPC3 properties of a native constitutively active Ca^{2+}-permeable cation channel in rabbit ear artery myocytes. *J Physiol* 2006; 571: 361–369.
13 Peel SE, Liu B, Hall IP. A key role for STIM1 in store operated calcium channel activation in airway smooth muscle. *Respir Res* 2006; 7: 119.
14 Ethier MF, Yamaguchi H, Madison JM. Effects of cyclopiazonic acid on cytosolic calcium in bovine airway smooth muscle cells. *Am J Physiol Lung Cell Mol Physiol* 2001; 281: L126–L133.
15 Ito S, Kume H, Yamaki K, *et al*. Regulation of capacitative and noncapacitative receptor-operated Ca^{2+} entry by ρ-kinase in tracheal smooth muscle. *Am J Respir Cell Mol Biol* 2002; 26: 491–498.
16 Ay B, Prakash YS, Pabelick CM, Sieck GC. Store-operated Ca^{2+} entry in porcine airway smooth muscle. *Am J Physiol Lung Cell Mol Physiol* 2004; 286: L909–L917.
17 Pabelick CM, Ay B, Prakash YS, Sieck GC. Effects of volatile anesthetics on store-operated Ca^{2+} influx in airway smooth muscle. *Anesthesiology* 2004; 101: 373–380.
18 Yamashita T, Kokubun S. Nonselective cationic currents activated by acetylcholine in swine tracheal smooth muscle cells. *Can J Physiol Pharmacol* 1999; 77: 796–805.
19 Tazzeo T, Zhang Y, Keshavjee S, Janssen LJ. Ryanodine receptors decant internal Ca^{2+} store in human and bovine airway smooth muscle. *Eur Respir J* 2008; 32: 275–284.
20 Bazan-Perkins B, Flores-Soto E, Barajas-Lopez C, Montano LM. Role of sarcoplasmic reticulum Ca^{2+} content in Ca^{2+} entry of bovine airway smooth muscle cells. *Naunyn Schmiedebergs Arch Pharmacol* 2003; 368: 277–283.
21 Flemming R, Xu SZ, Beech DJ. Pharmacological profile of store-operated channels in cerebral arteriolar smooth muscle cells. *British Journal of Pharmacology* 2003; 139: 955.
22 Terasawa K, Nakajima T, Iida H, *et al*. Nonselective cation currents regulate membrane potential of rabbit coronary arterial cell: modulation by lysophosphatidylcholine. *Circulation* 2002; 106: 3111–119.
23 Wilson SM, Mason HS, Smith GD, *et al*. Comparative capacitative calcium entry mechanisms in canine pulmonary and renal arterial smooth muscle cells. *J Physiol* 2002; 543: 917–931.
24 Ay B, Iyanoye A, Sieck GC, Prakash YS, Pabelick CM. Cyclic nucleotide regulation of store-operated Ca^{2+} influx in airway smooth muscle. *Am J Physiol Lung Cell Mol.Physiol* 2006; 290: L278–L283.
25 Albert AP, Large WA. A Ca^{2+}-permeable non-selective cation channel activated by depletion of internal Ca^{2+} stores in single rabbit portal vein myocytes. *J Physiol* 2002; 538: 717–728.
26 Albert AP, Piper AS, Large WA. Properties of a constitutively active Ca^{2+}-permeable non-selective cation channel in rabbit ear artery myocytes. *J Physiol* 2003; 549: 143–156.
27 Ng LC, Gurney AM. Store-operated channels mediate Ca^{2+} influx and contraction in rat pulmonary artery. *Circ Res* 2001; 89: 923–929.
28 Albert AP, Large WA. Activation of store-operated channels by noradrenaline *via* protein kinase c in rabbit portal vein myocytes. *J Physiol* 2002; 544: 113–125.
29 Halaszovich CR, Zitt C, Jungling E, Luckhoff A. Inhibition of TRP3 channels by lanthanides. block from the cytosolic side of the plasma membrane. *J Biol Chem* 2000; 275: 37423–37428.
30 Trepakova ES, Gericke M, Hirakawa Y, Weisbrod RM, Cohen RA, Bolotina VM. Properties of a native cation channel activated by ca^{2+} store depletion in vascular smooth muscle cells. *J Biol Chem* 2001; 276: 7782–7790.
31 Golovina VA, Platoshyn O, Bailey CL, *et al*. Upregulated TRP and enhanced capacitative Ca^{2+} entry in human pulmonary artery myocytes during proliferation. *Am J Physiol Heart Circ Physiol* 2001; 280: H746–H755.